arXiv:hep-ph/0306199v3 1 Dec 2004

Roper Resonance and $S_{11}(1535)$ from Lattice QCD

N. Mathur[a], Y. Chen[b], S.J. Dong[a], T. Draper[a], I. Horváth[a], F.X. Lee[c,d], K.F. Liu[a], and J.B. Zhang[e]

[a] *Dept. of Physics and Astronomy, University of Kentucky, Lexington, KY 40506*
[b] *Institute of High Energy Physics, Chinese Academy of Science, Beijing 100039, China*
[c] *Center for Nuclear Studies, Dept. of Physics, George Washington University, Washington, DC 20052*
[d] *Jefferson Lab, 12000 Jefferson Avenue, Newport News, VA 23606*
[e] *CSSM and Dept. of Physics and Mathematical Physics, University of Adelaide, Adelaide, SA 5005, Australia*

Abstract

Using the constrained curve fitting method and overlap fermions with the lowest pion mass at 180 MeV, we observe that the masses of the first positive and negative parity excited states of the nucleon tend to cross over as the quark masses are taken to the chiral limit. Both results at the physical pion mass agree with the experimental values of the Roper resonance ($N^{1/2+}(1440)$) and S_{11} ($N^{1/2-}(1535)$). This is seen for the first time in a lattice QCD calculation. These results are obtained on a quenched Iwasaki $16^3 \times 28$ lattice with $a = 0.2$ fm. We also extract the ghost $\eta' N$ states (a quenched artifact) which are shown to decouple from the nucleon interpolation field above $m_\pi \sim 300$ MeV. From the quark mass dependence of these states in the chiral region, we conclude that spontaneously broken chiral symmetry dictates the dynamics of light quarks in the nucleon.

The Roper resonance has been studied extensively, but its status as the first excited state of the nucleon with the same quantum numbers is intriguing. Although awarded four stars in the Particle Data Table, it is not as easily identifiable as other resonances. It does not show up as a peak in the cross sections in various experiments; rather its existence is revealed through phase shift analysis [1, 2]. Furthermore, the theoretical situation is in a quandary. First of all, it has been noted for a long time that it is rather unusual to have the first positive parity excited state lower than the negative parity excited state which is the $N^{1/2-}(1535)$ in the S_{11} πN channel. This is contrary to the excitation pattern in the meson sectors with either light or heavy quarks. This parity reversal has caused problems for the otherwise successful quark

models based on $SU(6)$ symmetry with color-spin interaction between the quarks [3] which cannot accommodate such a pattern. Realistic potential calculations with linear and Coulomb potentials [4] and the relativistic quark model [5] all predict the Roper to be ~ 100 – $200\,\mathrm{MeV}$ above the experimental value with the negative parity state lying lower. On the other hand, the pattern of parity reversal was readily obtained in the chiral soliton model like the Skyrme model via the small oscillation approximation to πN scattering [6]. Although the first calculation [7] of the original skyrmion gives rise to a breathing mode which is $\sim 200\,\mathrm{MeV}$ lower than the Roper resonance, it was shown later [8] that the introduction of the sixth order term, which is the zero range approximation for the ω meson coupling, changes the compression modulus, yielding better agreement with experiment for both the mass and width in πN scattering.

Since the quark potential model is based on the $SU(6)$ symmetry with residual color-spin interaction between the quarks, whereas the chiral soliton model is based on spontaneous broken chiral symmetry, their distinctly different predictions on the ordering of the positive and negative parity excited states may be a reflection of different dynamics as a direct consequence of the respective symmetry. This possibility has prompted the suggestion [9] that the parity reversal in the excited nucleon and Δ, in contrast to that in the excited Λ spectrum, is an indication that the inter-quark interaction of the light quarks is mainly of the flavor-spin nature rather than the color-spin nature (e.g. one-gluon exchange type.) This suggestion is supported in the lattice QCD study of "Valence QCD" [10] where one finds that the hyperfine splitting between the nucleon and Δ is largely diminished when the Z-graphs in the quark propagator are eliminated. This is an indication that the color-magnetic interaction is not the primary source of the inter-quark spin-spin interaction for light quarks. (The color-magnetic part, being spatial in origin, is unaffected by the truncation of Z-graphs in Valence QCD, which only affects the time part.) Yet, it is consistent with the Goldstone-boson-exchange picture which requires Z-graphs and leads to a flavor-spin interaction.

The failure of the $SU(6)$ quark model to delineate the Roper and its photoproduction has prompted the speculation that the Roper resonance may be a hybrid state with excited glue [11] or a $qqqq\bar{q}$ five quark state [12]. Thus, unraveling the nature of Roper resonance has direct bearing on our understanding of the quark structure and chiral dynamics of baryons, which is one of the primary missions at experimental facilities like Jefferson Lab.

Lattice QCD is perhaps the most desirable tool to adjudicate the theoretical controversy surrounding the issue. In fact, there have been several calculations to study the positive-parity excitation of the nucleon [13, 14, 15, 16, 17, 18]. However, they have not been able to probe the relevant low quark mass region while preserving chiral symmetry at finite lattice spacing (except Ref. [14] which uses the Domain Wall fermion). We employ the overlap fermion [19] on a large lattice which admits cal-

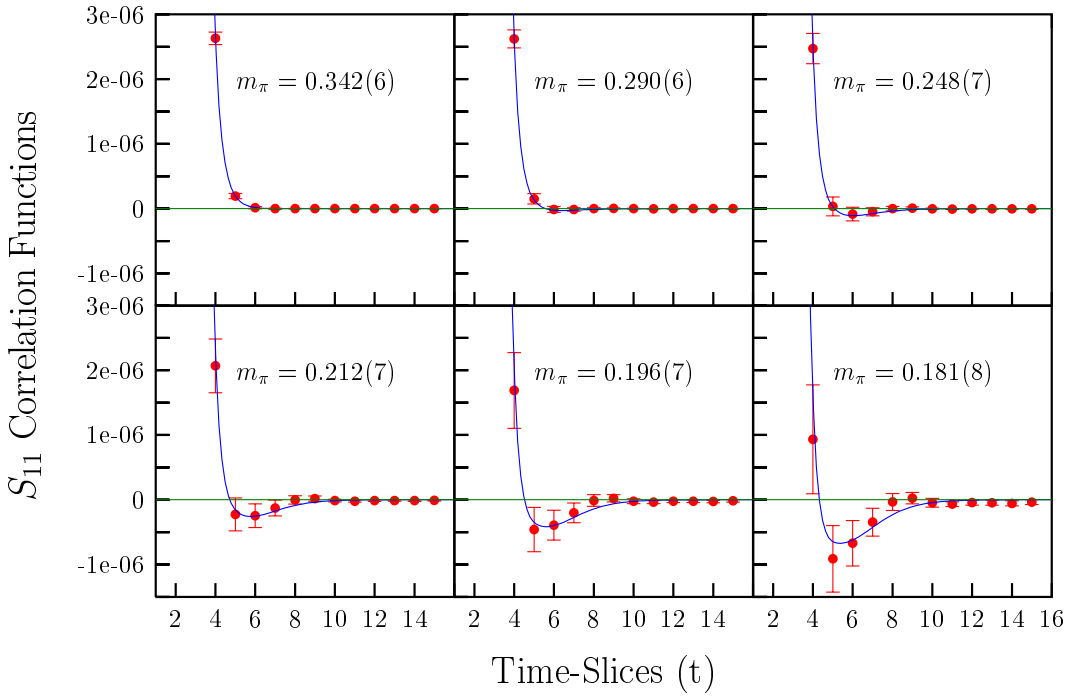

Figure 1: S_{11} correlators for six low quark masses. Negative dip of the correlators is an indication of the domination of the ghost $\eta' N$ state over the physical S_{11}. m_π are in GeV.

culations with realistically small quark masses [20] to study the chiral region. Since the controversy about the nature of Roper hinges on chiral symmetry, it is essential to have a fermion action which explicitly exhibits the correct spontaneously broken chiral symmetry.

Another difficulty of the calculation of the excited states in lattice QCD is that the conventional two-exponential fits are not reliable. Facing the uncertainty of the fitting procedure for the excited state, it has been suggested to use a non-standard nucleon interpolating field which vanishes in the non-relativistic limit [13, 14, 15, 16, 18], in the hope that it may have negligible overlap with the nucleon so that the Roper state can be seen more readily. However, the lowest state calculated with this interpolation field (2.2 GeV) [13, 14, 15, 16, 18] is much higher than the Roper state. Employing the maximum entropy method allows one to study the nucleon and its radial excitation with the standard nucleon interpolation field [17]. However, with the pion mass at $\sim$ 600 MeV, the nucleon radial excitation is still too high ($\sim$ 2 GeV). In order to have a reliable prediction of the excited state in lattice QCD calculations by way of addressing the above mentioned difficulties, we implement constrained curve fitting based on an empirical Bayes method. It has been advocated [21, 22] recently as a powerful tool which utilizes more data points while better controlling the systematics.

Since we adopt the quenched approximation, we should mention that there are quenched artifacts. Due to the absence of quark loops in quenched QCD, the would-be η' propagator involves only double η poles in hairpin diagrams. This leads to quenched chiral logs in hadron masses which are clearly observed and extracted from our recent lattice calculation of pion and nucleon masses [23]. Another quenched artifact is the contribution of ghost states in the hadron correlators. As first observed in the a_0 meson channel [24], the ghost S-wave $\eta'\pi$ state lies lower than a_0 for small quark mass. There is a similar situation with the excited state of the nucleon where the P-wave $\eta' N$ appears in the vicinity of the Roper. Since this is not clearly exhibited in the nucleon correlator where the nucleon is the lowest state in the channel and dominates the long-time behavior of the correlator, we can look at the parity partner of the nucleon ($N^{\frac{1}{2}-}$ or S_{11}) with $I = 1/2$. There, the lowest S-wave $\eta' N$ state with a mass close to the sum of the pion and nucleon masses can be lower than S_{11} for sufficiently low quark mass. Since the η – η coupling in the hairpin diagram is negative [24], one expects that the S_{11} correlator will turn negative at larger time separations as in the case of the a_0 [24]. In Fig. 1, we show the S_{11} correlators for 6 low quark cases with pion mass from $m_\pi = 181(8)\,\mathrm{MeV}$ to $m_\pi = 342(6)\,\mathrm{MeV}$. We see that for pion mass lower than $248(7)\,\mathrm{MeV}$, the S_{11} correlator starts to develop a negative dip at time slices beyond 4, and it is progressively more negative for smaller quark masses. This is a clear indication that the ghost $\eta' N$ state in the S-wave is dominating the correlator over the physical S_{11} which lies higher in mass.

One can calculate the one-loop hairpin diagram on a $L^3 \times T$ lattice which gives the following contribution to the zero-momentum nucleon correlator for the P-wave would-be η' loop

$$\begin{aligned} \Delta G_{NN}(t) &= -m_0^2 \frac{|Z|^2 T}{16 L^3} \sum_{\vec{p}} \frac{E_N + E_\pi + m_N}{E_N^2\, E_\pi^3} \\ &\times \frac{\vec{p}^{\,2}}{m_N^2} (1 + E_\pi t) e^{-(E_N + E_\pi)t}. \end{aligned} \tag{1}$$

Here $-m_0^2$ is the coupling between the would-be Goldstone bosons. However, this is not quite adequate to be used in the fitting because there is an interaction between the would-be η' and the nucleon which can lead to an energy which is different from $E_N + E_\pi$. Instead of modeling it with the re-summation of the hairpin diagram, as is done for the a_0 meson [24], we shall introduce these ghost states which are in the vicinity of the Roper and S_{11} with the form $W(1 + E_\pi t)e^{-E_{\eta' N} t}$. This has the same functional form as in Eq. (1). The $(1 + E_\pi t)$ pre-factor is preserved to reflect the double-pole nature of the hairpin diagram and the weight W is constrained to be negative to preserve the ghost nature of the state. The only exception is $E_{\eta' N}$ which is allowed to be different from but close to the non-interacting energy $E_N + E_\pi$. Being the energy of the interacting would-be η' and N state, it will be fitted to the data together with the negative weight W. Since we work in a finite box, the $\eta' N$ states are

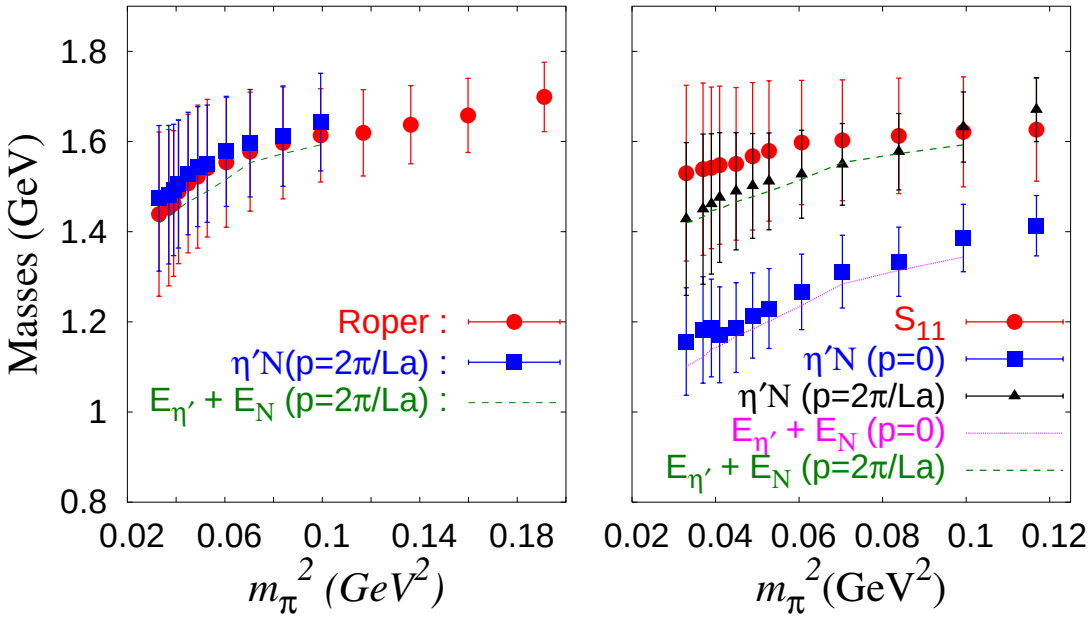

Figure 2: Roper (left) and S_{11} (right) masses with their associated $\eta' N$ ghost states.

discrete and they will be constrained to be near the energy of the two non-interacting particles, with discrete lattice momenta $p_n = \frac{2\pi n}{L}, n = 0, \pm 1, \cdots$.

With a constrained-curve fitting method [22], we develop an adaptive sequential way of extracting the priors from data at a smaller volume, i.e. $12^3 \times 28$. We fit the ground state first over a few large-time slices, and then use the fitted values as priors to constrain the ground state in a subsequent fit (which includes earlier time slices) of the excited state. We include the next excited states, one by one, constraining all previously fitted states to their most recently fitted values. For each new fit, we add one more earlier time slice and check if it is needed by comparing its contribution to the statistical error of the added time slice. When the time slices are exhausted, we use the resultant fit parameters as priors for a standard constrained-curve fit of the correlator on the larger $16^3 \times 28$ lattice. More details can be found in Ref. [22]. For the $\eta' N$ state, we make an appropriate adjustment to priors for $E_{\eta' N}$ and E_π due to the fact that the discrete momentum is inversely proportional to the spatial lattice size L. We find that the constraint to make W negative is crucial to obtain a fit with acceptable χ^2, especially for the case of the nucleon correlator where the Roper and the first $\eta' N$ state are nearly degenerate.

We shall report our results on $16^3 \times 28$ and $12^3 \times 28$ lattices with quenched Iwasaki gauge action and overlap fermions with a lattice spacing $a = 0.200(3)$ fm determined from $f_\pi(m_\pi)$. This makes our lattice sizes as large as 3.2 fm and 2.4 fm. At our lowest pion mass at 181(8) MeV, the finite volume error is estimated to be $\sim 2.7\%$ [23]. We first present the Roper and S_{11} masses for the $16^3 \times 28$ lattice with their associated ghost $\eta' N$ states in the P-wave and S-wave respectively. They are plotted as a

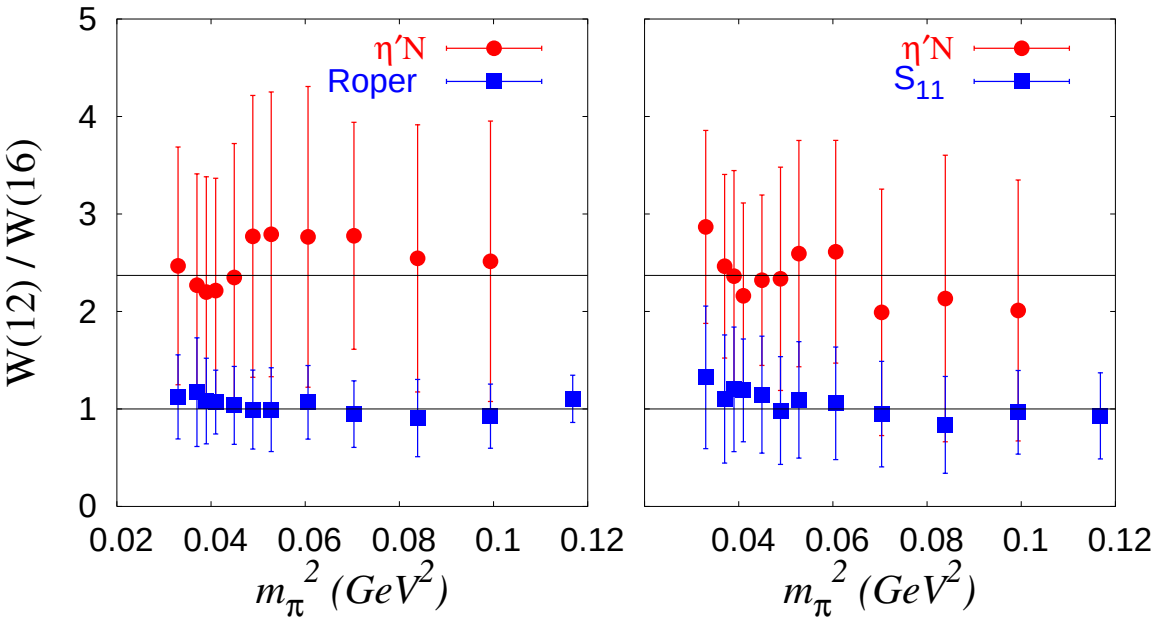

Figure 3: Ratio of spectral weights from 12^3 to 16^3 lattices for Roper and P-wave $\eta' N$ (left) and S_{11} and S-wave $\eta' N$ (right).

function of m_π^2 in Fig. 2. We see in Fig. 2 (left) that the $\eta' N$ state ($p = 2\pi/L$) and the Roper are nearly degenerate; they are resolved when the weight for the $\eta' N$ is constrained to be negative. Fig. 2 (right) shows that the $p = 0$ S-wave $\eta' N$ lies lower than S_{11}, and below $m_\pi \sim 316\,\mathrm{MeV}$ the $p = 2\pi/L$ $\eta' N$ state also becomes lower than S_{11}. The dashed line in Fig. 2 (left) is the mass for the non-interacting would-be η' and N which lies below the fit of the $\eta' N$ state. This shows that there is a repulsive interaction of about 50 MeV between the would-be η' and N in the P-wave. The corresponding non-interacting $\eta' N$ states, represented by the solid line ($p = 0$) and the dashed line ($p = 2\pi/L$) in Fig. 2 (right), are closer to the interacting $\eta' N$ states with $\sim 10 - 50\,\mathrm{MeV}$ repulsion in this case.

To verify that the $\eta' N$ state can be separated from the physical Roper and S_{11}, we examine the ratio of the spectral weights for the Roper (respectively, the S_{11}) and the $\eta' N$ from the $12^3 \times 28$ lattice to that on the $16^3 \times 28$ lattice. (See Fig. 3.) The ratio for the Roper (S_{11}) is consistent with unity which is expected for a one-particle state; whereas, the corresponding ratios for the $\eta' N$ states are more consistent with the ratio of the three volumes $V_3(16)/V_3(12) = 2.37$ which reflects the volume dependence of the two-particle scattering state.

In Fig. 4, we display the weight of the $\eta' N$ state and those of the Roper and S_{11}. The weight for the Roper is essentially constant (Fig. 4 (left)) and that of S_{11} decreases as the pion mass increases and reaches a constant for $m_\pi > 400\,\mathrm{MeV}$ (Fig. 4 (right)). The negative weight of the $\eta' N$ is 3 orders of magnitude smaller than

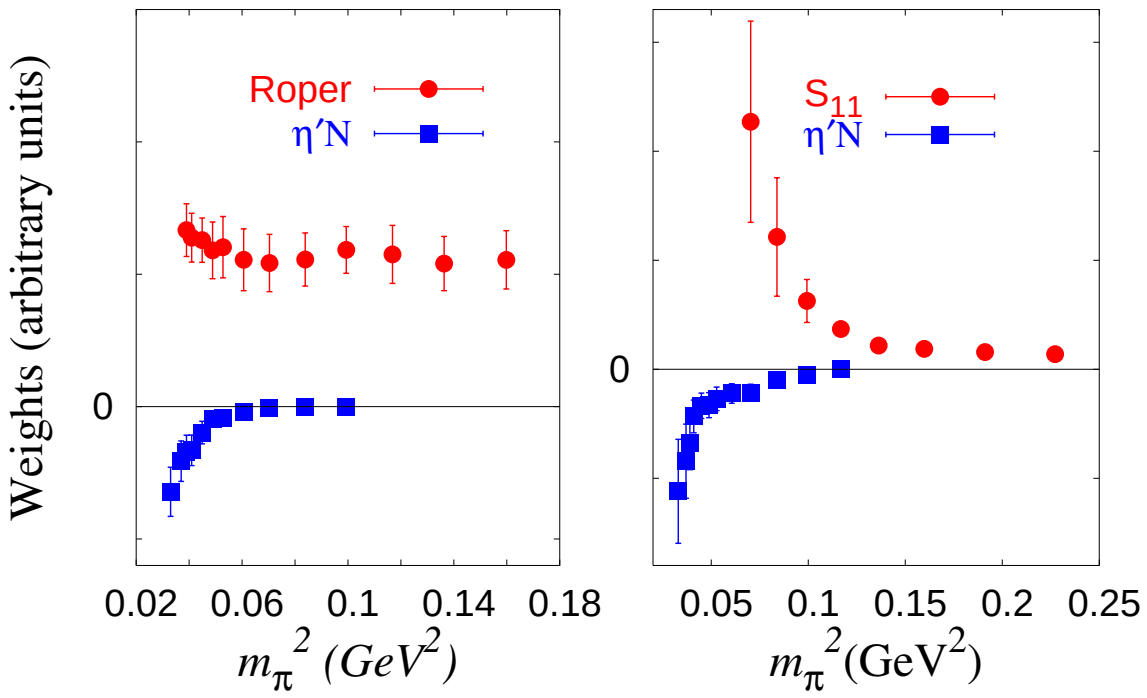

Figure 4: Weights of Roper and $\eta' N$ (left), and S_{11} and $\eta' N$ (right). They are in arbitrary units.

the Roper above $m_\pi = 266\,\mathrm{MeV}$ in the nucleon channel and $m_\pi = 320\,\mathrm{MeV}$ in the S_{11} channel. This decoupling means that the two-particle intermediate state $\eta' N$ is not produced by the three-quark nucleon interpolating field $\chi_N^\dagger$ so that the matrix element $\langle \eta' N | \chi_N^\dagger | 0 \rangle$ is zero. This confirms our earlier study of Valence QCD [10] which suggests that, for higher quark mass, the $SU(6)$ symmetry prevails which explains why the valence quark model with color-spin interaction works well. However, for light quarks, it is chiral symmetry which dictates the dynamics via the Z-graphs. This is to be manifested as the meson loops as well as meson exchanges between quarks in the chiral quark model of the baryon [25]. The present study suggests that this transition occurs in the region $m_\pi \sim 300\,\mathrm{MeV}$. We should point out that the fact that the $\eta' N$ ghost states are separated out from the physical $S_{11}(1535)$ in our fitting relies on the fact that the ghost state has a different functional form from that of the physical state and its weight is negative. When the dynamical fermion calculation is available with realistically light quarks, these $\eta' N$ ghost states will turn into physical ηN and $\eta' N$ states. Since $S_{11}(1535)$ is close to the ηN threshold and both have the same functional form, i.e. $W\, e^{-mt}$, it would be difficult to separate them with a fitting procedure based on one interpolation field.

Finally, we plot the nucleon, Roper and S_{11} in Fig. 5 as a function of m_π^2. We see that for heavy quarks ($m_\pi \geq 800$ MeV), the Roper, S_{11}, and nucleon splittings

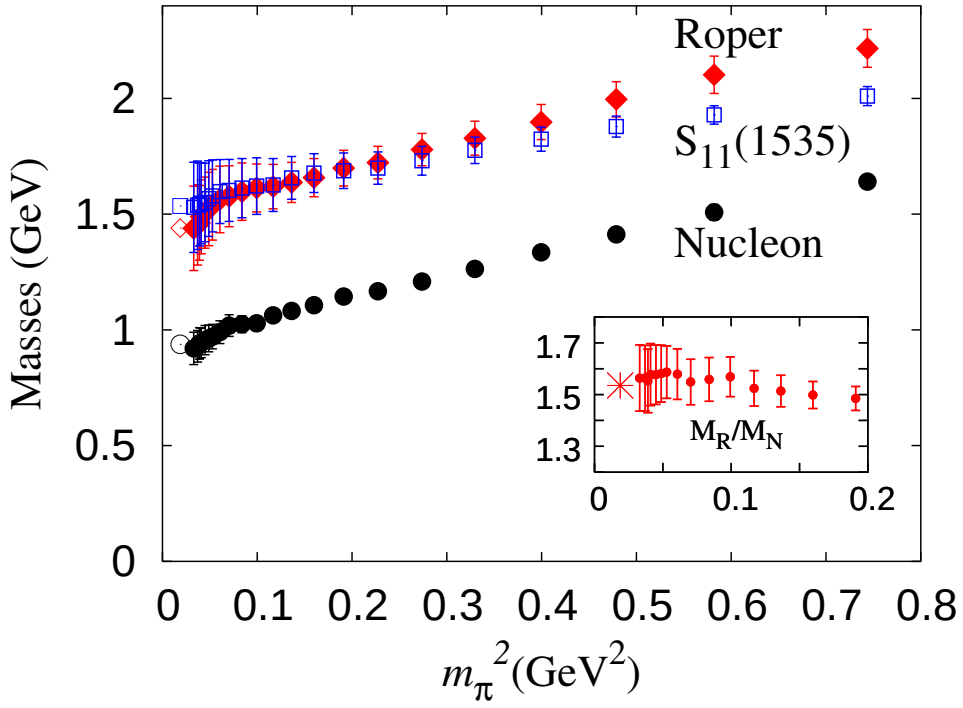

Figure 5: Nucleon, Roper, and S_{11} masses in GeV as a function of m_π^2. The experimental values are indicated by the corresponding open symbols.

are like those of the heavy quarkonium. When the quark mass becomes lighter, the Roper and S_{11} have a tendency to coincide and possibly cross over. More statistics are needed to clarify this point. However, we have plotted as the insert in Fig. 5 the ratio of Roper to nucleon as a function of $m_\pi^2(\mathrm{GeV}^2)$ which has a smaller error (by $\sim 40\%$) than the Roper mass itself. It shows that the Roper is consistent with the experimental value near the physical pion mass. The chiral behavior of the nucleon mass is analyzed in more detail with the inclusion of the $m_\pi \log(m_\pi)$ term in [23]. Here, we shall simply use the form $C_0 + C_{1/2} m_\pi + C_1 m_\pi^2$ to extrapolate the Roper and S_{11} to the physical pion mass. The resultant nucleon mass of 928(56) MeV, Roper at 1462(157) MeV, and S_{11} at 1554(65) MeV are consistent with the experimental values ($m_N = 939\,\mathrm{MeV}$, $m_R \approx 1440\,\mathrm{MeV}$, and $m_{S_{11}} \approx 1535\,\mathrm{MeV}$). This suggests that a successful description of the Roper resonance depends not so much on the use of the dynamical quarks, but that most of the essential physics is captured by using light quarks to ensure the correct chiral behavior.

To conclude, with the help of constrained curve fitting (which allows fitting of the excited states including the ghost $\eta' N$ states) and the overlap fermion (which admits calculations with realistically small quark masses), we are able to study the Roper and S_{11} closer to the chiral limit than before. The physical Roper and S_{11} are distinguished from the ghost two-particle intermediate states ($\eta' N$) by checking their volume dependence of the weights as a function of the pion mass. We observe the

tendency for the Roper and S_{11} to cross over (with the caveat of large errors) at the low m_π region. This is consistent with the thesis that the order reversal between the Roper and $S_{11}(1535)$ compared to the heavy quark system is caused by the flavor-spin interaction between the quarks due to Goldstone boson exchanges [9]. We support the notion that there is a transition from heavy quarks (where the $SU(6)$ symmetry supplemented with color-spin interaction for the valence quarks gives a reasonable description) to light quarks (where the dynamics is dictated by chiral symmetry). It is suggested that this transition occurs at $m_\pi \sim 300 - 400\,\mathrm{MeV}$ for the nucleon.

This work is partially supported by DOE Grants DE-FG05-84ER40154 and DE-FG02-95ER40907. We wish to thank A. Bernstein, G.E. Brown, L. Glozman, D.O. Riska, and S. Sasaki for useful discussions.

References

[1] R.A. Arndt *et al.*, Phys. Rev. **C52**, 2120 (1995).

[2] G. Hohler, *piN* Newsletter, **9**, 1 (1993).

[3] See, e.g. S. Capstick and W. Roberts, Prog. Part. Nucl. Phys. 45, S241 (2000), [nucl-th/0008028].

[4] K.F. Liu and C.W. Wong, Phys. Rev. **D28**, 170 (1983).

[5] S. Capstick and N. Isgur, Phys. Rev. **D34**, 2809 (1986).

[6] See, for example, M. Mattis in Chiral Solitons, ed. K.F. Liu (World Scientific, 1987), p. 171.

[7] K.F. Liu, J.S. Zhang, and G.R.E. Black, Phys. Rev. **D30**, 2015 (1984); J. Breit and C.R. Nappi, Phys. Rev. Lett. **53**, 889 (1984).

[8] U.B. Kaulfuss and U-G. Meissner, Phys. Lett. **154B**, 193 (1985).

[9] L.Y. Glozman and D.O. Riska, Phys. Rep. **268**, 263 (1996).

[10] K.F. Liu, S.J. Dong, T. Draper, D. Leinweber, J. Sloan, W. Wilcox, R. Woloshyn, Phys. Rev. **D59** 112001 (1999).

[11] T. Barnes and F.E. Close, Phys. Lett. **123B**, 221 (1983); Z. Li, Phys. Rev. **D44**, 2841 (1991); C.E. Carlson and N.C. Mukhopadhyay, Phys. Rev. Lett. **67**, 3745 (1991).

[12] O. Krehl, C. Hanhart, S. Krewald, J. Speth, Nucl. Phys. **C62**, 025207 (2000).

[13] F.X. Lee and D. Leinweber, Nucl. Phys. (Proc. Suppl.) **B73**, 258 (1999); F.X. Lee, Nucl. Phys. (Proc. Suppl.) **B94**, 251 (2001).

[14] S. Sasaki, T. Blum, and S. Ohta, Phys. Rev. **D65**, 074503 (2002).

[15] D.G. Richards et al., (LHP/QCDSF/UKQCD Collaboration), Nucl. Phys. (Proc. Suppl.) **B109**, 89 (2002).

[16] W. Melnitchouk et al., hep-lat/0202022.

[17] S. Sasaki, K. Sasaki, T. Hatsuda, and M. Asakawa, Lattice 2002, [hep-lat/0209059]; S. Sasaki, Prog. Theor. Phys. Suppl. 151, 143 (2003), [nucl-th/0305014].

[18] R. Edwards, U. Heller, D. Richards, Lattice 2002, [hep-lat/0303004].

[19] H. Neuberger, Phys. Lett. **B 417**, 141 (1998).

[20] S.J. Dong, F.X. Lee, K.F. Liu, and J.B. Zhang, Phys. Rev. Lett. **85**, 5051 (2000).

[21] G.P. Lepage et al., Nucl. Phys. (Proc. Suppl.) **106**, 12 (2002).

[22] Y. Chen, S.D. Dong, T. Draper, I. Horvath, K.F. Liu, N. Mathur, S. Tamhankar, C. Srinivasan, F.X. Lee, J.B. Zhang, hep-lat/0405001.

[23] Y. Chen, S.J. Dong, T. Draper, I. Horváth, F.X. Lee, K.F. Liu, N. Mathur, and J.B. Zhang, Phys. Rev. **D70**, (2004) 034502, [hep-lat/0304005].

[24] W. Bardeen, A. Duncan, E. Eichten, N. Isgur, H. Thacker, Phys. Rev. **D65**, 014509 (2002).

[25] K.F. Liu, S.J. Dong, T. Draper, J. Sloan, W. Wilcox, R.M. Woloshyn, Phys. Rev. **D61**, 118502 (2000).